Crystalline-State Reaction of Cobaloxime Complexes by X-ray Exposure. 13. A Stepwise Structure Analysis of the Concerted Process of Racemization

Yuji Ohashi,*† Yasuko Tomotake, Akira Uchida, and Yoshio Sasada

Contribution from the Laboratory of Chemistry for Natural Products, Tokyo Institute of Technology, Nagatsuta 4259, Midori-ku, Yokohama 227, Japan. *Received February 27, 1985*

Abstract: A new type of crystalline-state racemization by X-ray exposure has been found in the crystal of [(*R*)-1-cyanoethyl]bis(dimethylglyoximato)(3-methylpyridine)cobalt(III). The cell dimensions gradually changed, but the noncentrosymmetric space group, $P2_12_12_1$, remained unaltered during the racemization. The changes of *a* and *c* followed first-order kinetics whereas those of *b* and *V* had maxima at the intermediate stage. After 900 h the change was within experimental error. The structure was determined at six stages. The crystal has two molecules in the asymmetric units. In the early stages, both of the chiral cyanoethyl groups of the two molecules, A and B cn groups, were gradually inverted into the opposite configuration. The rate of the inversion of the B cn group was about twice as large as that of the A cn group. After 400 h, the crystal was completely racemized but the conversion of the two groups continued; the B cn group was further inverted whereas the A cn group was gradually restored to the original configuration. The racemization process observed at 343 K was very similar to that at 293 K. However, the rate of the inversion of the B cn group at 343 K became smaller than that at 293 K whereas the A cn group had approximately the same rate at the two temperatures. These results are well-explained by the shape and volume of the reaction cavities for the A and B cn groups.

It has been found that the chiral 1-cyanoethyl (cn) group in crystals of some bis(dimethylglyoximato)cobalt, cobaloxime, complexes is racemized by X-ray exposure without degradation of the crystallinity.[1] In the previous paper,[2] we reported that the modes of the racemization were divided into three classes. The crystals in the first class contain one molecule per asymmetric unit and the ordered chiral cn group is converted into the disordered racemate.[3,4] In the second and thrid classes, each crystal has two molecules per asymmetric unit, which are related by a pseudoinversion center. One of the chiral groups of the two molecules in the crystal of the second class is transformed into the opposite configuration and the crystallographic inversion center appears between the two molecules.[5-7] For the crystal of the third class, both of the chiral groups of the two independent molecules are converted into the disordered racemate and the pseudoinversion center becomes a crystallographic one.[2]

Recently we have found that the crystals of the cobaloxime complex with the chiral cyanoethyl (cn) group and 3-methylpyridine as axial ligands (*R*-cn-3mepy, Figure 1) are also racemized by X-ray exposure but the racemization process does not belong to any of the above classes. Moreover, the racemization does not follow the first-order kinetics as observed in the above crystals and the racemization rate decreases with increase in temperature. The structures were determined at several intermediate stages, which is essential for the elucidation of the reaction mechanism not obeying first-order kinetics. To our knowledge, this is the first example of the stepwise structure analysis applied successfully to such a complicated solid-state reaction.

Experimental Section

R-cn-3mepy was prepared in a way similar to that reported previously.[8] Orange plate-like crystals were obtained from an aqueous methanol solution. The Rigaku AFC-4 diffractometer and Mo Kα radiation monochromated by graphite were used. The accurate cell dimensions were determined by means of the least-squares technique with 20 reflections in the range of $18° < 2\theta < 28°$.

Crystal data at the initial stage at 293 K are as follows: $C_{17}H_{25}CoN_6O_4$; fw = 436.4; a = 11.696 (4) Å, b = 38.34 (2) Å, c = 9.215 (3) Å; V = 4132 (3) Å^3; space group $P2_12_12_1$; Z = 8; d_x = 1.407 g cm^{-3}; μ(Mo Kα) = 8.09 cm^{-1}.

On exposure to the conventional Mo Kα radiation (45 kV, 25 mA),[9] the unit-cell dimensions of the crystal were gradually changed. Figure 2 shows the variation of a, b, c, and V with exposure time, which was obtained with use of a crystal of 0.4 × 0.3 × 0.1 mm. After about 900 h, the changes were within the experimental error. The exposure time was recorded by a clock which ran when the X-ray window-shutter was open. The changes of a and c are well-explained by the first-order kinetics, whereas those of b and V have maxima at the intermediate stage. The space group $P2_12_12_1$ remained unaltered.

Three-dimensional intensity data were collected at the six stages denoted as I to VI in Figure 2, using one crystal of 0.6 × 0.5 × 0.2 mm. For each stage intensities of reflections in the range of $2\theta \leq 50°$ were measured by means of an ω scan with a scanning rate of 4°(ω) min^{-1} and a scan width of 1.0°. Stationary background counts were accumulated for 5 s before and after each scan. The exposure time necessary for the data collection at each stage was about 39 h. In the course of the data collection the orientation matrix was redetermined if the intensities of three monitor reflections varied by more than 10σ. The reflections with $|F_o| \geq 3\sigma(F_o)$ were used for the structure determination. No corrections for absorption or extinction were made ($\mu r \simeq 0.5$). The integrated intensities of reflections at the early intermediate stages decreased to a considerable extent and then increased slowly and turned to about 90% the initial values. A similar intensity variation has been observed in the related crystals reported previously.[3]

In order to examine the temperature dependence of the change, a crystal of 0.4 × 0.3 × 0.2 mm was warmed at 343 K on the diffractometer with use of the hot-air-flow method. The three-dimensional intensity data were collected at the three stages denoted as I′ to III′ in Figure 2. The variation of the cell dimensions was measured during and between the data collections. Although the unit cell expanded anisotropically at 343 K, a similar trend of the cell variation with time was observed for the two temperatures as shown in Figure 2. After 900 h, the values of a, b, c, and V were 11.569 (3), 38.28 (1), and 9.354 (2) Å and 4142 (2) Å^3, respectively. On cooling to 293 K, they became essentially the same as those at stage VI.

† Present address: Department of Chemistry, Ochanomizu University, Otsuka 2-1-1, Bunkyo-ku, Tokyo 112, Japan.

(1) Ohashi, Y.; Sasada, Y. *Nature (London)* **1977**, *267*, 142-144.
(2) Tomotake, Y.; Uchida, A.; Ohashi, Y.; Sasada, Y.; Ohgo, Y; Baba, S. *Isr. J. Chem.* **1985**, *25*, 327-333.
(3) Ohashi, Y.; Yanagi, K.; Kurihara, T.; Sasada, Y.; Ohgo, Y. *J. Am. Chem. Soc.* **1981**, *103*, 5805-5812.
(4) Ohashi, Y.; Sasada, Y.; Ohgo, Y. *Chem. Lett.* **1978**, 743-746.
(5) Ohashi, Y.; Yanagi, K.; Kurihara, T.; Sasada, Y.; Ohgo, Y. *J. Am. Chem. Soc.* **1982**, *104*, 6353-6359.
(6) Ohashi, Y.; Uchida, A.; Sasada, Y.; Ohgo, Y. *Acta Crystallogr., Sect. B* **1983**, *B39*, 54-61.
(7) Uchida, A.; Ohashi, Y.; Sasada, Y.; Ohgo, Y.; Baba, S. *Acta Crystallogr., Sect. B* **1984**, *B40*, 478-483.
(8) Ohgo, Y.; Takeuchi, S.; Natori, Y.; Yoshimura, J.; Ohashi, Y.; Sasada, Y. *Bull. Chem. Soc. Jpn.* **1981**, *54*, 3093-3099.
(9) It was observed that the rate of reaction was significantly dependent on the X-ray wavelength, when two crystals cut from a big one were exposed to Cu Kα and Mo Kα radiations. Detailed discussion will appear elsewhere.

0002-7863/86/1508-1196$01.50/0

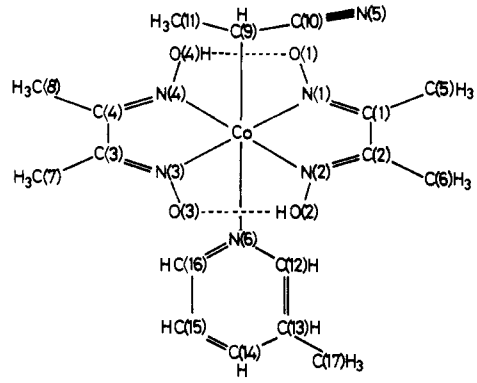

Figure 1. [(*R*)-1-Cyanoethyl](3-methylpyridine)cobaloxime.

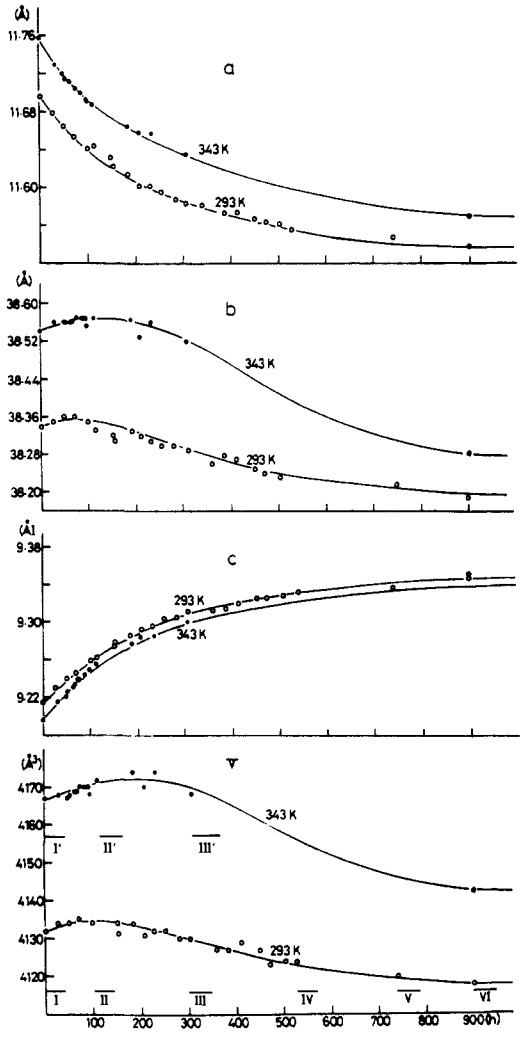

Figure 2. The change of the unit-cell dimensions at 293 K (circles) and at 343 K (black dots). Three-dimensional intensity data were collected at stages I to VI at 293 K, I′ to III′ at 343 K, and III′ at 293 K.

The structure at stage I was solved by using the program MULTAN 78[10] and refined by the restrained least-squares method with the program SHELX 76,[11] to avoid parameter interaction between the two crystallographically independent molecules, A, and B. Most of the hydrogen atoms were found on the difference map and the others were located geometrically. In the final refinement, the non-hydrogen and hydrogen atoms were refined with anisotropic and isotropic temperature factors,

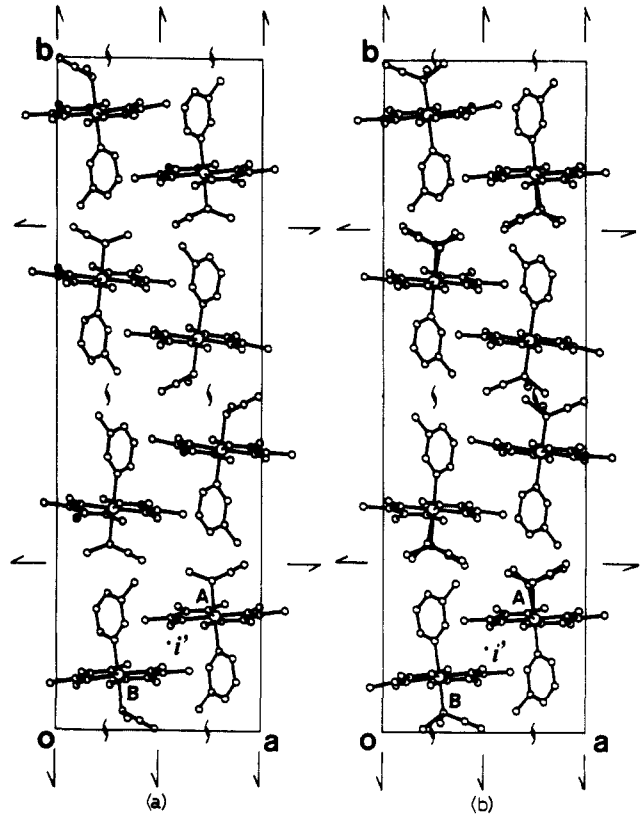

Figure 3. Crystal structures viewed along the *c* axis at stages (a) I and (b) VI. The local pseudoinversion center is indicated by *i*′.

respectively, and all the bond distances between non-hydrogen atoms were loosely restrained to have the mean value of the corresponding ones of the related molecules and the bond distances including the hydrogen atoms were fixed to be 1.00 Å. The weighting scheme used was $\{(\sigma(F_o))^2 + CF_o^2\}^{-1}$, where $C = 0.001\,039$. The maximum residual peak around the Co atoms, P_m, and that between the molecules, P_i, on the final difference map were 0.49 and 0.34 eÅ^{-3}, respectively. Although the absolute configuration of the cn group must be R since the complex was prepared from [*R*-1-cn]((*S*)-α-methylbenzylamine)cobaloxime, it was confirmed by the anomalous-dispersion technique with Cu Kα radiation. The structure at the final stage VI was also solved with the MULTAN 78 program and refined by the restrained least-squares method. The cn groups of the A and B molecules revealed the disordered structures. The occupancy factors of the newly appearing atoms with opposite configuration were also refined, the isotropic temperature factors being fixed to have the same values as those of the corresponding atoms of the original groups. The other conditions of the least-squares refinement are the same as those at stage I. Both of the structures at stages I and VI are essentially the same except for the inverted A and B cn groups, whose occupancy factors are 0.25 (1) and 0.84 (2), respectively. The structures at the other stages II, III, IV, and V were refined in a similar way, starting from the average structure at stages I and VI. No significant changes were observed in the structures of the intermediate stages, except for the occupancy factors of the disordered cn groups. The positions of all the hydrogen atoms were unable to be located at stages II to VI and the isotropic temperature factors were not refined. At stage II′, only the parameters for non-hydrogen atoms were refined, since it was difficult to locate the positions of the hydrogen atoms. The refinement of stage III′ was not satisfactorily carried out. The intensity data were collected at 293 K after the data collection of stage III′ at 343 K, using the same crystal. The structure determined at 293 K, stage III′(293 K), was essentially the same as that at 343 K. The occupancy factors of the inverted methyl groups of the B cn groups were 0.49 (4) and 0.49 (3) for stages III′ and III′(243 K), respectively. Hereafter the structure at stage III′(293 K) is used instead of that at stage III′. The cell dimensions and the experimental details for each stage are summarized in Table I. Atomic scattering factors including the anomalous-dispersion terms were taken from ref 12. The calculations were carried out on a FACOM-HITAC system M-180 computer at this Institute. Final atomic param-

(10) Main, P.; Hull, S. E.; Lessinger, L.; Germain, G.; Declercq, J. P.; Woolfson, M. M. MULTAN 78 (a system of computer programs for the automatic solution of crystal structures from X-ray diffraction data); University of York, England, and Louvain, Belgium, 1978.

(11) Sheldrick, G. M. (1976) SHELX 76 (a program for crystal structure determination); Univerisity of Cambridge, England, 1976.

(12) "International Tables for X-ray Crystallography"; Kynoch Press: Birmingham, England, 1974; Vol. IV, pp 72–150.

Table I. Unit Cell Dimensions and Details of Refinement at Each Stage[a]

	293 K					
	I	II	III	IV	V	VI
a	11.696 (4)	11.644 (3)	11.584 (3)	11.552 (2)	11.548 (2)	11.537 (2)
b	38.34 (2)	38.33 (1)	38.29 (1)	38.22 (1)	38.22 (1)	38.18 (1)
c	9.215 (3)	9.262 (2)	9.311 (2)	9.332 (2)	9.334 (1)	9.347 (1)
V	4132 (3)	4134 (2)	4130 (2)	4121 (2)	4120 (1)	4117 (1)
N	3591	2744	2800	3487	3523	3650
R	0.056	0.075	0.094	0.103	0.081	0.069
N_p	587	555	533	496	545	566
C	0.001039	0.001689	0.001592	0.001805	0.001789	0.004705
P_m	0.49	0.47	0.56	0.69	0.57	0.56
P_i	0.34	0.50	0.56	0.79	0.80	0.76
(A')			0.33 (2)	0.26 (1)	0.29 (1)	0.25 (1)
(B')		0.27 (2)	0.55 (2)	0.73 (2)	0.88 (2)	0.84 (2)

	343 K			
	I′	II′	III′	III′(293 K)
a	11.758 (6)	11.687 (3)	11.635 (4)	11.577 (5)
b	38.54 (3)	38.57 (1)	38.52 (2)	38.30 (2)
c	9.196 (3)	9.255 (2)	9.300 (3)	9.301 (3)
V	4167 (4)	4172 (2)	4168 (3)	4124 (3)
N	2469	2659	2383	2303
R	0.072	0.085		0.102
N_p	587	470		501
C	0.000860	0.00597		0.001549
P_m	0.58	0.37		0.75
P_i	0.51	0.51		0.75
(A')				0.33 (2)
(B')		0.21 (3)		0.49 (3)

[a] N is the number of observed reflections; N_p is the number of parameters; C is the factor in the weighting scheme; P_m is the maximum residual peak around the Co atoms on the final difference map; P_i is the maximum residual peak between the molecules; (A') is the occupancy factor of the inverted A cn group; (B') is the occupancy factor of the inverted B cn group. The inverted A cn group at the stages II, II′ and III′ was undetectable on the difference map.

eters for non-H atoms at stages I and VI at 293 K are given in Tables II and III, respectively.[13]

Results and Discussion

Crystal Structure. Crystal structure viewed along the c axis at stage I is shown in Figure 3a. Except for the cyanoethyl group, the two crystallographically independent molecules A and B, are related by a local inversion center, i' at the coordinates 0.5435, 0.1264, 0.2650. The cyanoethyl groups of the A molecules, A cn groups, are connected by a 2_1 axis to form a ribbon along the a axis, whereas the B cn groups make a ribbon along the c axis by another 2_1 axis. There are no unusually short contacts between the molecules.

Figure 3b shows the crystal structure viewed along the c axis at stage VI. Both of the A and B cn groups are converted into the disordered racemates. The local inversion center does not change to a crystallographic one and the noncentrosymmetric space group $P2_12_12_1$ is conserved. This is in marked contrast to the crystalline-state racemization observed in the third class, in which the pseudoinversion center becomes a crystallographic one after the racemization.

Since the C—C≡N bonds of A and B molecules in the crystal of R-cn-3mepy are not antiparallel to each other as observed in the crystals of the second and third classes, the pseudoinversion center cannot change to a crystallographic one without rotation of the A or B cn group by about 180° around the Co–C bond. For the crystalline-state racemization of the methoxycarbonylethyl (mce) groups in the crystals of [R-1-mce](4-chloropyridine)cobaloxime[14] and [R-1-mce](pyridine)cobaloxime methanol solvate,[15] the bulkier mce group than the cn group can rotate by about 180° around the Co–C bond and the crystallographic inversion center appears between the two crystallographically independent molecules at high temperatures. The cn group in the R-cn-3mepy crystal is inverted without rotating around the Co–C bond even at 343 K. This is probably due to the fact that the pseudoinversion center does not meet the crystal symmetry and the void space around the cn group is too small for the rotation.

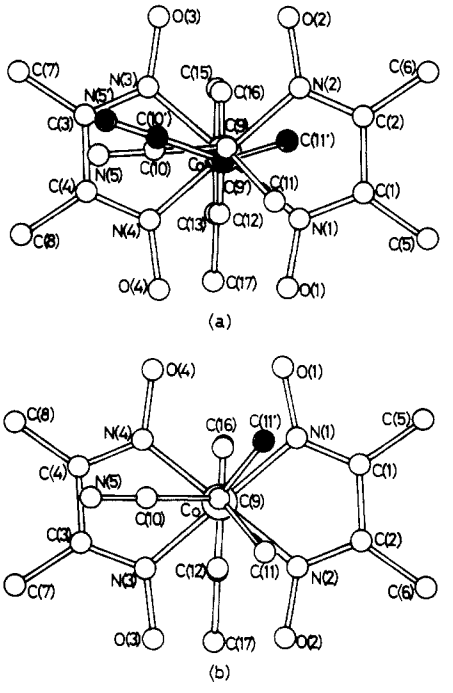

Figure 4. The structures of (a) A and (b) B molecules viewed along the normal to the mean plane of cobaloxime. The shaded atoms are newly appearing ones in the process of the racemization.

Molecular Structure. Figure 4 shows the A and B molecules at stage VI viewed along the normal to the cobaloxime plane. Selected bond distances and torsion angles at stages I and VI are listed in Table IV. The newly appearing cn group with the S

(13) See paragraph at end of paper regarding supplementary material.
(14) Kurihara, T.; Ohashi, Y.; Sasada, Y.; Ohgo, Y. *Acta Crystallogr., Sect. B* **1983**, *B38*, 243–250.
(15) Kurihara, T.; Uchida, A.; Ohashi, Y.; Sasada, Y.; Ohgo, Y. *J. Am. Chem. Soc.* **1984**, *106*, 5718–5724.

Table II. Final Atomic Coordinates for Non-Hydrogen Atoms at Stage I

atom	*x*	*y*	*z*	B_{eq} (Å^2)
Co (A)	0.27880 (7)	0.32935 (2)	0.01235 (8)	3.00 (2)
N (1A)	0.1184 (4)	0.3353 (1)	0.0192 (6)	3.8 (1)
N (2A)	0.2451 (5)	0.3204 (1)	−0.1844 (5)	4.1 (2)
N (3A)	0.4386 (4)	0.3237 (1)	0.0042 (6)	4.1 (2)
N (4A)	0.3092 (4)	0.3368 (1)	0.2113 (5)	3.7 (1)
O (1A)	0.0622 (4)	0.3437 (1)	0.1406 (5)	5.1 (1)
O (2A)	0.3253 (5)	0.3109 (1)	−0.2806 (5)	5.6 (2)
O (3A)	0.4932 (4)	0.3155 (1)	−0.1184 (6)	5.5 (2)
O (4A)	0.2275 (4)	0.3431 (1)	0.3091 (5)	5.5 (1)
C (1A)	0.0626 (5)	0.3317 (2)	−0.1018 (7)	3.9 (2)
C (2A)	0.1373 (5)	0.3221 (2)	−0.2212 (6)	4.2 (2)
C (3A)	0.4931 (5)	0.3270 (2)	0.1269 (7)	4.7 (2)
C (4A)	0.4175 (6)	0.3347 (2)	0.2474 (6)	4.4 (2)
C (5A)	−0.0622 (5)	0.3360 (2)	−0.1129 (11)	6.5 (3)
C (6A)	0.0971 (9)	0.3147 (2)	−0.3706 (7)	6.8 (3)
C (7A)	0.6179 (6)	0.3210 (2)	0.1422 (13)	7.8 (3)
C (8A)	0.4526 (9)	0.3370 (2)	0.4030 (7)	7.2 (3)
C (9A)	0.2634 (5)	0.2766 (1)	0.0463 (6)	4.6 (2)
C (10A)	0.3542 (6)	0.2638 (2)	0.1400 (8)	5.4 (2)
C (11A)	0.1519 (7)	0.2637 (2)	0.1041 (13)	9.1 (4)
N (5A)	0.4196 (6)	0.2527 (2)	0.2165 (9)	8.2 (3)
N (6A)	0.2980 (4)	0.3813 (1)	−0.0288 (5)	3.3 (1)
C (12A)	0.2495 (5)	0.4059 (1)	0.0542 (7)	4.1 (2)
C (13A)	0.2637 (5)	0.4417 (1)	0.0290 (7)	4.6 (2)
C (14A)	0.3310 (6)	0.4513 (2)	−0.0840 (7)	5.0 (2)
C (15A)	0.3799 (5)	0.4269 (2)	−0.1711 (7)	4.7 (2)
C (16A)	0.3634 (5)	0.3920 (1)	−0.1404 (6)	4.1 (2)
C (17A)	0.2057 (7)	0.4673 (2)	0.1285 (11)	6.8 (3)
Co (B)	0.30827 (7)	0.08210 (2)	0.54236 (8)	3.00 (2)
N (1B)	0.1493 (4)	0.0739 (1)	0.5316 (5)	3.8 (1)
N (2B)	0.2726 (4)	0.0885 (1)	0.7401 (5)	3.8 (1)
N (3B)	0.4676 (4)	0.0880 (1)	0.5550 (5)	3.6 (1)
N (4B)	0.3434 (4)	0.0755 (1)	0.3446 (5)	4.1 (2)
O (1B)	0.0967 (4)	0.0661 (1)	0.4058 (5)	5.3 (1)
O (2B)	0.3508 (4)	0.0975 (1)	0.8409 (4)	5.0 (1)
O (3B)	0.5211 (4)	0.0944 (1)	0.6803 (5)	4.9 (1)
O (4B)	0.2639 (4)	0.0677 (1)	0.2430 (5)	5.7 (2)
C (1B)	0.0928 (5)	0.0755 (2)	0.6525 (7)	4.4 (2)
C (2B)	0.1654 (5)	0.0842 (2)	0.7756 (6)	4.4 (2)
C (3B)	0.5239 (5)	0.0860 (2)	0.4335 (7)	4.6 (2)
C (4B)	0.4509 (5)	0.0781 (2)	0.3089 (7)	4.4 (2)
C (5B)	−0.0315 (5)	0.0675 (2)	0.6655 (11)	6.7 (3)
C (6B)	0.1235 (8)	0.0859 (2)	0.9289 (7)	6.8 (3)
C (7B)	0.6514 (5)	0.0891 (2)	0.4258 (10)	6.4 (3)
C (8B)	0.4931 (8)	0.0720 (2)	0.1581 (8)	6.8 (3)
C (9B)	0.3303 (5)	0.0294 (1)	0.5771 (7)	4.7 (2)
C (10B)	0.4160 (6)	0.0147 (2)	0.4813 (8)	5.7 (2)
C (11B)	0.3556 (9)	0.0181 (2)	0.7296 (9)	8.4 (3)
N (5B)	0.4870 (7)	0.0031 (2)	0.4136 (9)	9.6 (3)
N (6B)	0.2856 (4)	0.1341 (1)	0.5063 (5)	3.6 (1)
C (12B)	0.3367 (5)	0.1584 (1)	0.5858 (6)	3.9 (2)
C (13B)	0.3216 (6)	0.1941 (1)	0.5639 (7)	4.9 (2)
C (14B)	0.2526 (6)	0.2044 (1)	0.4522 (7)	4.8 (2)
C (15B)	0.1972 (6)	0.1806 (2)	0.3683 (7)	5.5 (2)
C (16B)	0.2168 (5)	0.1457 (1)	0.3987 (6)	4.3 (2)
C (17B)	0.3849 (8)	0.2201 (2)	0.6600 (11)	7.2 (3)

configuration has a different conformation in the two molecules. The conformations of the cn groups with the *R* configuration and those of the 3-methylpyridine ligands are approximately the same as the corresponding ones at the initial stage. The bond distances and bond angles at the initial stage are in good agreement with those of the related complexes containing pyridine,[5] 4-pyridinecarbonitrile,[6] and 4-methylpyridine[7] as axial ligands.

The crystal and molecular structures at stages I′, II′, and III′ at 343 K are essentially the same as those at stages I, II, and III at 293 K, respectively, except for the occupancy factors of the cn groups.

Rate of Racemization. The above observation in the successive structure analyses with a crystal at 293 K clearly indicates that the crystal is racemized by X-rays; the photochemical process has been discussed in the previous paper.[3,5] The changes of *a* and *c* shown in Figure 2 are well-explained by the first-order kinetics. The rate constants, k_a and k_c, and the average values, k_{av}, were

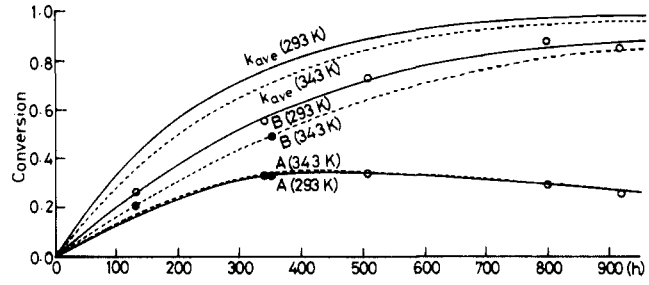

Figure 5. The changes of the occupancy factors of the newly appearing A and B cn groups with exposure time at 293 and 343 K. The upper two first-order kinetic curves expressed as $\{1 - \exp(-k_{av}t)\}$ indicate the variation of the cell dimensions, *a* and *c*, at the two temperatures where k_{av} is the average rate constant and *t* is the exposure time. After the 900-h exposure at 343 K, the crystal was cooled to 293 K and the structure was determined. The same occupancy factors for the two cn groups as those at stage VI were obtained.

calculated to be 1.12×10^{-6}, 1.23×10^{-6}, and 1.18×10^{-6} s^{-1} at 293 K and 0.96×10^{-6}, 1.01×10^{-6}, and 0.99×10^{-6} s^{-1} at 343 K, respectively. These values, however, are not regarded as the rate of the racemization, since the changes of *b* and *V* are significantly deviated from the first-order kinetic curves. Similar non-first-order kinetic curves have been observed for the crystalline-state dimerization of 2-benzyl-5-benzylidenecyclopentanone.[16] In order to obtain the reaction rate, the structures were determined on the basis of the three-dimensional intensity data at the six stages at 293 K and at the three stages at 343 K. The occupancy factors of the newly appearing A and B cn groups with the inverted configuration were derived at each stage.

Figure 5 shows the changes of the occupancy factors with exposure time. The change of the B cn group seems to follow the first-order kinetics and the ratio of the inverted group reaches 0.90 after 900 h. The rate constants, k_B, were calculated to be 0.66×10^{-6} and 0.56×10^{-6} s^{-1} at 293 and 343 K, respectively. The conversion of the A cn group, on the other hand, has a maximum (0.35) at 400 h and becomes 0.25 at 900 h. Although the crystal is fully racemized by X-ray exposure for aboout 400 h, the conversion of the A and B cn groups still continues after 400 h. The B cn group appears to be completely inverted and the A cn group is probably restored to the original configuration after infinite exposure. The contraction of the unit cell, which would bring about a gain in potential energy, could probably be a motivating force for the whole change.

Reaction Cavity. In order to explain the difference in the rate of conversion of the A and B cn groups, the cavities for the A and B cn groups were drawn as defined in a previous paper.[6] Figure 6 shows the cavities at stage I.[17] The cavity for the A cn group, A cavity, viewed along the normal to the cobaloxime plane is significantly narrower than the B cavity. Such a difference in the shapes of the cavities well explains the different conformations of the inverted cn groups with the *S* configuration after the racemization as shown in Figure 4. The volumes of the cavities were calculated to be 10.24 and 14.29 Å^3 for the A and B cn groups, respectively. Since the B cavity is greater than the A cavity, the rate of the B cn group is larger than that of the A cn group in the early stages.

Figure 7 illustrates the two cavities at stage I′ at 343 K. The shapes of the cavities are very similar to the corresponding ones at 293 K. The volumes of the cavities are 10.84 and 12.79 Å^3 for the A and B cn groups, respectively. Surprisingly the volume of the B cavity decreases with the increase in temperature, although the unit cell expands by 35Å^3 at 343 K. The A cavity, on the other hand, has approximately the same volume at the two temperatures.

(16) Nakanishi, H.; Jones, W; Thomas, J. M.; Hursthouse, M. B.; Motevalli, M. *J. Phys. Chem.* **1981**, *85*, 3636–3642.

(17) The volume of the cavity severely depends on the positions of the hydrogen atoms of the neighboring molecules. Since the positions of all the hydrogen atoms were not able to be located at stages II to VI, the precise volumes of the cavities at the stages were unobtainable.

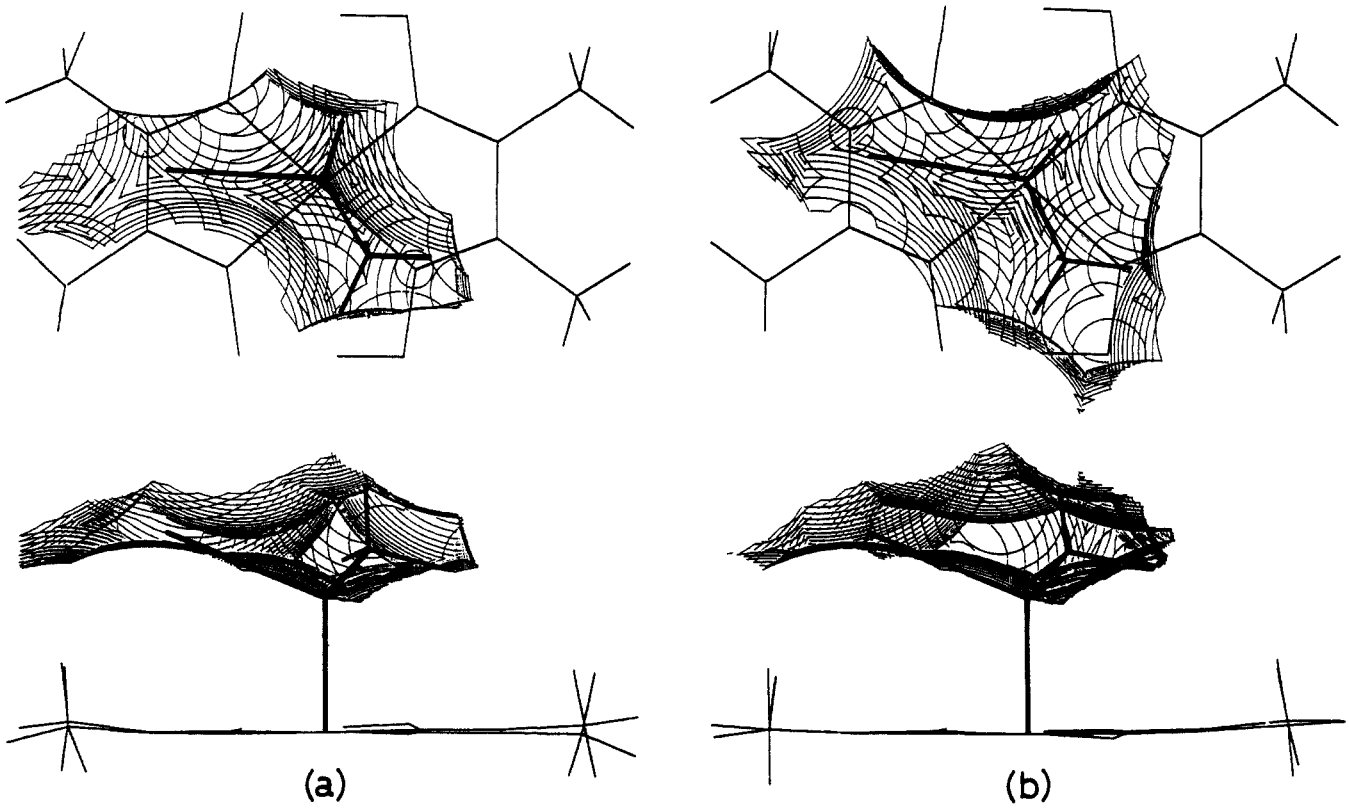

Figure 6. The cavities for (a) A and (b) B cn groups at stage I, viewed along the normal to the cobaloxime plane (top) and the short axis of cobaloxime (bottom). The contours are drawn in sections separated by 0.1 Å.

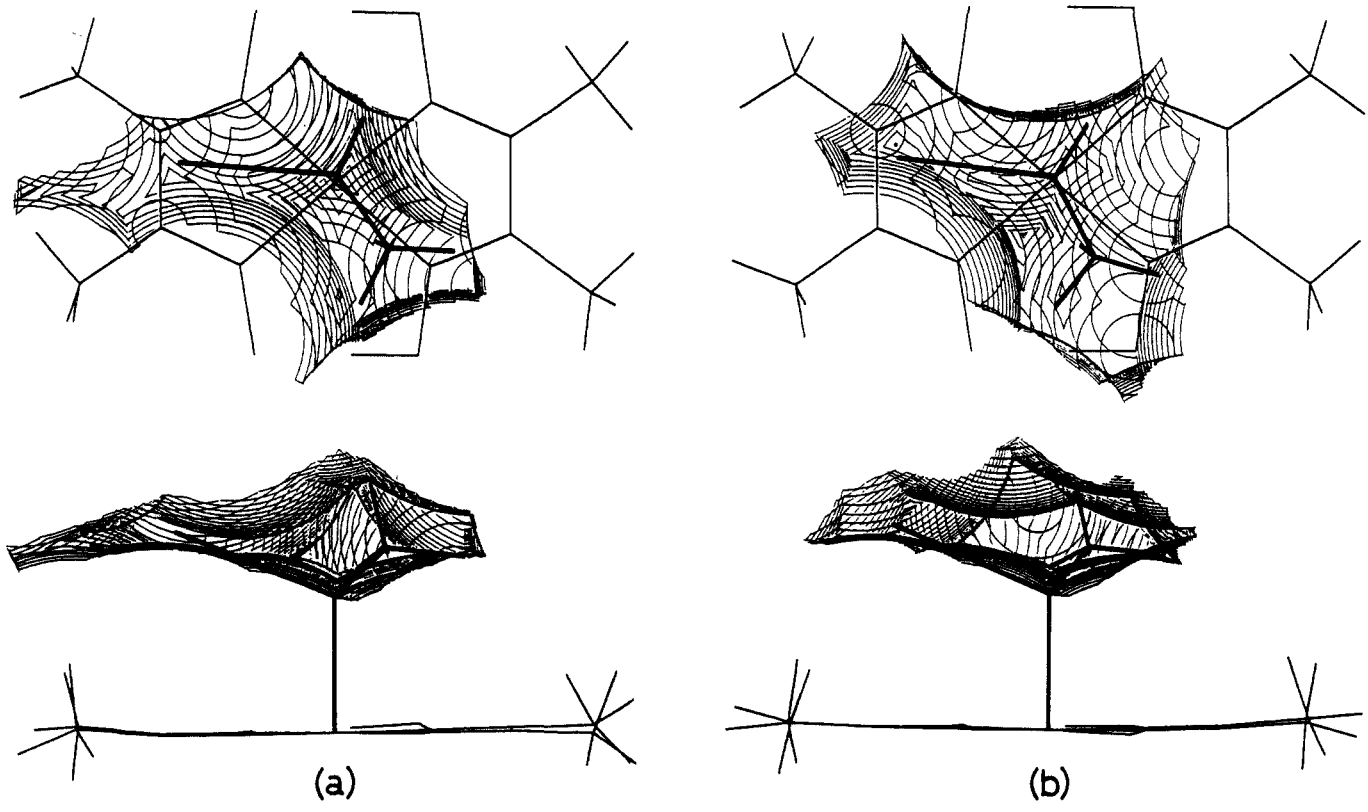

Figure 7. The cavities for (a) A and (b) B cn groups at the stage VI, drawn in the same way as Figure 5.

The rate of the inversion of the B cn group at 343 K is significantly smaller than that at 293 K, whereas approximately the same rates were observed at the two temperatures for the A cn group. The positive correlation between the reaction rate and the volume of the reaction cavity holds good for the present crystal, too. It must be emphasized that the reaction rate decreases with the increase in temperature if the cavity for the reactive group becomes smaller at high temperatures than at room temperature.

Reaction Mechanism. The modes of the crystalline-state racemization were divided into three classes. Parts a and b in Fugure 8 schematically show the racemization of the second and third classes. One of the two crystallographically independent cn groups is converted into the opposite configuration in the second class, whereas both cn groups are transformed to the disordered racemate

Table III. Final Atomic Coordinates for Non-Hydrogen Atoms at Stage VI

atom	*x*	*y*	*z*	*B* or B_{eq} (Å²)[a]
Co (A)	0.24769 (8)	0.33073 (2)	0.02332 (11)	3.00 ⟨4⟩
N (1A)	0.0851 (4)	0.3352 (2)	0.0305 (7)	3.7 ⟨2⟩
N (2A)	0.2143 (6)	0.3224 (2)	−0.1723 (6)	4.1 ⟨2⟩
N (3A)	0.4098 (4)	0.3258 (2)	0.0149 (7)	4.0 ⟨2⟩
N (4A)	0.2788 (5)	0.3373 (2)	0.2197 (6)	4.1 ⟨2⟩
O (1A)	0.0284 (6)	0.3426 (2)	0.1529 (7)	5.5 ⟨2⟩
O (2A)	0.2975 (6)	0.3142 (2)	−0.2689 (6)	5.4 ⟨2⟩
O (3A)	0.4659 (6)	0.3186 (2)	−0.1069 (8)	5.6 ⟨2⟩
O (4A)	0.1946 (6)	0.3421 (2)	0.3180 (6)	5.7 ⟨2⟩
C (1A)	0.0294 (6)	0.3318 (2)	−0.0890 (8)	4.2 ⟨2⟩
C (2A)	0.1057 (6)	0.3238 (2)	−0.2079 (8)	4.2 ⟨2⟩
C (3A)	0.4644 (7)	0.3290 (2)	0.1360 (8)	4.4 ⟨2⟩
C (4A)	0.3871 (7)	0.3361 (2)	0.2561 (8)	4.7 ⟨3⟩
C (5A)	−0.0984 (7)	0.3342 (3)	−0.0969 (16)	6.5 ⟨4⟩
C (6A)	0.0621 (10)	0.3159 (3)	−0.3531 (9)	6.2 ⟨3⟩
C (7A)	0.5915 (7)	0.3244 (4)	0.1474 (19)	7.8 ⟨5⟩
C (8A)	0.4269 (14)	0.3378 (4)	0.4060 (10)	7.6 ⟨4⟩
N (6A)	0.2636 (4)	0.3831 (1)	−0.0121 (6)	3.1 ⟨1⟩
C (12A)	0.2113 (7)	0.4067 (2)	0.0716 (9)	4.2 ⟨2⟩
C (13A)	0.2272 (8)	0.4427 (2)	0.0529 (9)	4.8 ⟨2⟩
C (14A)	0.2944 (8)	0.4539 (3)	−0.0574 (11)	5.5 ⟨3⟩
C (15A)	0.3479 (9)	0.4301 (2)	−0.1425 (12)	5.1 ⟨3⟩
C (16A)	0.3321 (7)	0.3946 (2)	−0.1192 (9)	4.4 ⟨2⟩
C (17A)	0.1604 (11)	0.4678 (2)	0.1523 (12)	6.9 ⟨4⟩
Co (B)	0.27847 (8)	0.08204 (3)	0.52654 (11)	3.10 ⟨4⟩
N (1B)	0.1161 (5)	0.0744 (2)	0.5136 (7)	4.3 ⟨2⟩
N (2B)	0.2414 (6)	0.0862 (2)	0.7220 (5)	4.0 ⟨2⟩
N (3B)	0.4396 (4)	0.0888 (2)	0.5404 (6)	3.3 ⟨2⟩
N (4B)	0.3164 (5)	0.0769 (2)	0.3325 (6)	4.0 ⟨2⟩
O (1B)	0.0643 (6)	0.0685 (2)	0.3876 (7)	5.7 ⟨2⟩
O (2B)	0.3206 (6)	0.0929 (2)	0.8234 (6)	5.2 ⟨2⟩
O (3B)	0.4924 (5)	0.0943 (2)	0.6660 (7)	5.3 ⟨2⟩
O (4B)	0.2357 (6)	0.0698 (2)	0.2315 (6)	5.5 ⟨2⟩
C (1B)	0.0607 (7)	0.0740 (3)	0.6350 (8)	5.0 ⟨3⟩
C (2B)	0.1341 (6)	0.0812 (2)	0.7576 (8)	4.5 ⟨2⟩
C (3B)	0.4974 (6)	0.0875 (2)	0.4218 (7)	4.0 ⟨2⟩
C (4B)	0.4251 (6)	0.0802 (2)	0.2987 (7)	4.0 ⟨2⟩
C (5B)	−0.0640 (8)	0.0653 (4)	0.6447 (19)	7.7 ⟨5⟩
C (6B)	0.0908 (11)	0.0831 (3)	0.9084 (10)	6.6 ⟨3⟩
C (7B)	0.6261 (7)	0.0902 (3)	0.4172 (15)	6.1 ⟨3⟩
C (8B)	0.4691 (11)	0.0746 (3)	0.1508 (10)	6.3 ⟨3⟩
C (9B)	0.3035 (6)	0.0291 (2)	0.5581 (10)	5.1 ⟨3⟩
C (10B)	0.4090 (7)	0.0170 (2)	0.4873 (13)	7.5 ⟨4⟩
N (5B)	0.4892 (7)	0.0068 (2)	0.4334 (14)	10.0 ⟨4⟩
N (6B)	0.2551 (5)	0.1350 (1)	0.4972 (6)	3.6 ⟨2⟩
C (12B)	0.3085 (7)	0.1587 (2)	0.5795 (8)	4.1 ⟨2⟩
C (13B)	0.2960 (7)	0.1947 (2)	0.5575 (8)	4.5 ⟨2⟩
C (14B)	0.2232 (7)	0.2045 (3)	0.4489 (10)	5.4 ⟨3⟩
C (15B)	0.1667 (8)	0.1814 (2)	0.3630 (10)	5.4 ⟨3⟩
C (16B)	0.1862 (8)	0.1464 (2)	0.3913 (9)	4.6 ⟨3⟩
C (17B)	0.3600 (10)	0.2205 (3)	0.6526 (13)	6.9 ⟨4⟩
C (9A)	0.2384 (7)	0.2761 (2)	0.0473 (10)	4.7 (1)
C (10A)	0.3257 (7)	0.2653 (2)	0.1536 (11)	4.7 (1)
C (11A)	0.1182 (6)	0.2629 (2)	0.0910 (11)	4.7 (1)
N (5A)	0.3913 (7)	0.2550 (2)	0.2327 (9)	4.7 (1)
C (9′A)	0.2192 (16)	0.2798 (3)	0.0749 (29)	4.7 (5)
C (10′A)	0.3229 (19)	0.2624 (3)	0.1288 (31)	4.7 (5)
C (11′A)	0.1450 (20)	0.2570 (3)	−0.0173 (35)	4.7 (5)
N (5′A)	0.4028 (18)	0.2483 (4)	0.1647 (29)	4.7 (5)
C (11B)	0.2879 (30)	0.0143 (6)	0.7048 (26)	8.8 (4)
C (11′B)	0.2030 (7)	0.0047 (2)	0.5314 (18)	8.8 (4)

[a] The atoms with angle brackets were refined anisotropically and others were done isotropically.

in the third class. In both classes the pseudoinversion center, *i*′, becomes a crystallographic one, *i*. The racemization process of the present crystal is also schematically shown in Figure 8c. Although the A and B molecules are related by a pseudoinversion center, the center does not meet the crystal symmetry and is not converted to a crystallographic one after the racemization. In early stages the A and B cn groups were gradually inverted into the opposite configuration. The rate of the inversion of the B cn group was about twice as large as that of the A cn group. After 400 h, the crystal was completely racemized but the conversion

Table IV. Selected Bond Distances (Å) and Torsional Angles (deg) Stages I and VI

	I	VI
Co(A)–N(1A)	1.891 (5)	1.885 (6)
Co(A)–N(2A)	1.887 (6)	1.896 (7)
Co(A)–N(3A)	1.883 (6)	1.881 (7)
Co(A)–N(4A)	1.889 (5)	1.887 (7)
Co(A)–N(6A)	2.042 (5)	2.037 (5)
Co(A)–C(9A)	2.054 (6)	2.10 (1)
Co(A)–C(9′A)		2.03 (3)
Co(B)–N(1B)	1.888 (5)	1.900 (11)
Co(B)–N(2B)	1.885 (5)	1.883 (7)
Co(B)–N(3B)	1.881 (5)	1.882 (6)
Co(B)–N(4B)	1.885 (5)	1.876 (7)
Co(B)–N(6B)	2.039 (5)	2.058 (6)
Co(B)–C(9B)	2.062 (7)	2.064 (9)
C(10A)–C(9A)–Co(A)–N(3A)	+38.3 (5)	+45.5 (7)
C(10′A)–C(9′A)–Co(A)–N(3A)		+18.0 (20)
C(10B)–C(9B)–Co(B)–N(4B)	+31.8 (5)	+44.3 (7)
C(11B)–C(9B)–Co(B)–N(2B)	−22.0 (6)	−0.8 (16)
C(11′B)–C(9B)–Co(B)–N(1B)		+11.8 (9)
N4(A)–Co(A)–N(6A)–C(12A)	−46.1 (5)	−47.1 (6)
N(3B)–Co(B)–N(6B)–C(12B)	−46.9 (5)	−46.1 (6)

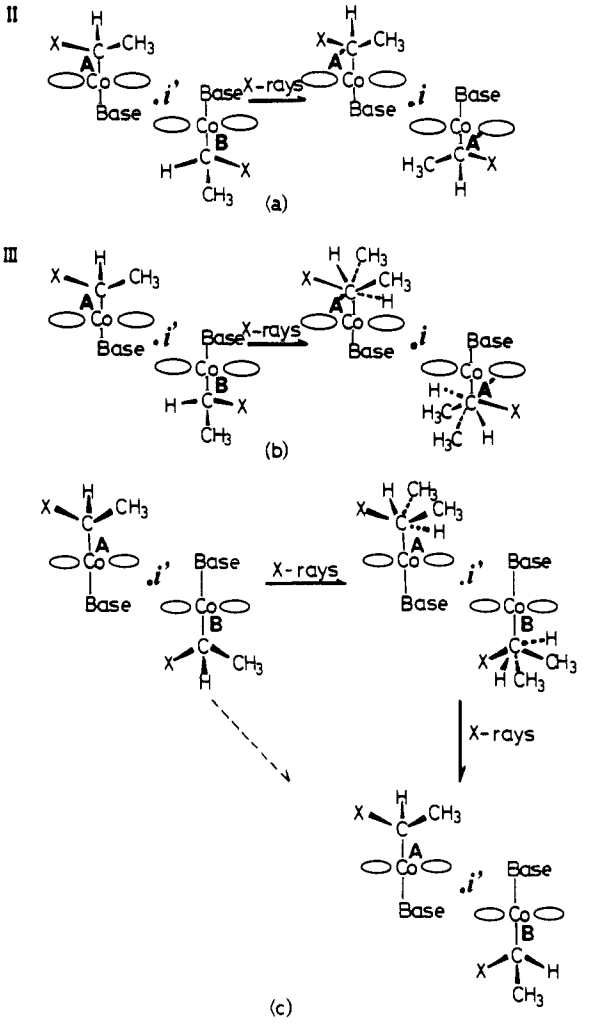

Figure 8. Schematic drawing of the racemization process observed in the crystals of (a) the second class, (b) the third class, and (c) *R*-cn-3mepy.

of the two groups continued; the B cn group was further inverted whereas the A cn group was gradually restored to the original configuration. After infinite exposure the B cn group will be completely inverted and the A cn group will have the original configuration.

Table V gives the volumes of the A and B cavities in the crystals of the second and third classes and of the present complex. The B cavity of the present crystal has enough volume for the inversion

Table V. The Volume of the Cavity (Å^3) for the Cyanoethyl Group in the Related Crystals

complex[a]	A cn group	B cn group	ref
second class			
R-cn-py	8.89	11.34	5
R-cn-cnpy	7.97	10.37	6
R-cn-4mepy	11.05	12.61	7
third class			
R-cn-dpmp	17.08	18.01	2
present crystal			
R-cn-3mepy (293 K)	10.24	14.29	
R-cn-3mepy (343 K)	10.84	12.79	

[a] *R*-cn-py, *R*-cn-cnpy, *R*-cn-4mepy, and *R*-cn-dpmp contain pyridine, 4-pyridinecarbonitrile, 4-methylpyridine, and diphenylmethylphosphine as axial ligands instead of 3-methylpyridine.

whereas the volume of the A cavity is a little smaller than those of the other reactive groups. The reason why not only B but also A cn groups can be inverted at the initial stage can be explained by the fact that the crystalline-field to produce the inversion symmetry in the present crystal would be weaker than that in the crystals of the second class since the pseudoinversion center does not meet the crystal symmetry in the former crystal. However, either of the A and B cavities is too small to accommodate the disordered racemate and the molecules would be more favorably packed when the two cn groups have opposite configurations. This causes the reinversion of the A cn group, and finally all the B cn groups will be converted to the opposite configuration and all the A cn groups to the original configuration.

In a crystal of the second class, on the other hand, some portion of the A cn groups would be inverted at the intermediate stages. However, the reinversion of the A cn group may occur so fast that the intermediate state as shown in Figure 8c cannot be detected. For a crystal of the third class, both of the A and B cavities have enough volume to accommodate the disordered racemate and the contraction of the unit cell would be prohibited because of the bulky phosphine ligand. The disordered structure would gain in entropy.

In the present crystal, the interaction between the two cn groups is not so strong or not so weak that we were able to analyze directly the concerted change of the two groups at several intermediate stages. Such a stepwise structure analysis, which we call "dynamical structure analysis", would be a powerful tool in elucidating the reaction mechanism. Further quantitative study on the mechanism is in progress.

Acknowledgment. This work was partly supported by a Grant-in-Aid for Scientific Research from the Ministry of Education, Science and Culture, Japan (No. 59470126).

Supplementary Material Available: Tables of atomic parameters for non-H and H atoms, anisotropic thermal parameters for non-H atoms, and the observed and calculated structure factors at the nine stages I to VI and I′ to III′ except the atomic parameters for non-H atoms at the stages I and VI (143 pages). Ordering information is given on any current masthead page.

Crown Thioether Chemistry. Synthetic, Structural, and Physical Studies of the Cu(II) and Cu(I) Complexes of Hexathia-18-crown-6

JudithAnn R. Hartman and Stephen R. Cooper*

Contribution from the Inorganic Chemistry Laboratory, University of Oxford, South Parks Road, Oxford OX1 3QR, England, and the Department of Chemistry, Harvard University, Cambridge, Massachusetts 02138. *Received June 4, 1985*

Abstract: The copper(II) and copper(I) complexes of hexathia-18-crown-6 have been synthesized and characterized by electron paramagnetic resonance, electrochemical, and X-ray diffraction methods. The copper(II) complex, [Cu·(hexathia-18-crown-6)](picrate)$_2$, crystallizes in the triclinic system, space group $P\bar{1}$, with a = 6.661 (1) Å, b = 9.669 (2) Å, and c = 13.594 (3) Å, α = 84.84 (2)°, β = 75.52 (2)°, and γ = 76.80 (2)°, and Z = 1. The copper(I) complex, [Cu·(hexathia-18-crown-6)](BF$_4$), crystallizes in the orthorhombic system, space group $Pna2_1$, with a = 10.855 (4) Å, b = 18.592 (7) Å, c = 10.137 (4) Å, and Z = 4. The centrosymmetric copper(II) complex adopts an axially elongated octahedral geometry, with Cu-S(eq) distances of 2.323 (1) and 2.402 (1) Å and a Cu-S(ax) distance of 2.635 (1) Å. Glasses at 77 K of [Cu·(hexathia-18-crown-6)](picrate)$_2$ in 1:1 nitromethane-toluene yield an EPR spectrum with g_x = 2.028, g_y = 2.035, and g_z = 2.119, $A_\parallel$ = 0.0153 cm^{-1}, and $A_\perp \approx$ 0.0019 cm^{-1}. The copper(I) complex assumes a distorted four-coordinate geometry that can be considered as derived from a linear two-coordinate complex by addition of two thioether groups; Cu-S distances are 2.253 (2) and 2.245 (2), and 2.358 (2) and 2.360 (2) Å, respectively, for these two types of ligands. Cyclic voltammetry shows that the Cu(II) and Cu(I) complexes are connected by an essentially reversible one-electron redox process at very high potential: +0.96 V vs. NHE.

Elucidation of the structure of the blue copper proteins plastocyanin[1,2] and azurin[3] has demonstrated thioether coordination to the copper ion but left unresolved the origin of the peculiar electronic structure of the metal-containing active site.[4,5] To clarify the relationship between electronic and molecular structure numerous studies have been directed toward synthesis of low molecular weight copper complexes with coordination spheres similar to those now known for the proteins.[6-19] Two fundamental issues have been stirred by the unusual redox, optical, and electron paramagnetic resonance characteristics of these proteins: First, to what extent, if any, are these properties attributable simply

* Address correspondence to this author at the University of Oxford.

(1) Colman, P. M.; Freeman, H. C.; Guss, J. M.; Murata, M.; Norris, V. A.; Ramshaw, J. A. M.; Venkatappa, M. P. *Nature (London)* **1978**, *272*, 319-324.
(2) Guss, J. M.; Freeman, H. C. *J. Mol. Biol.* **1983**, *169*, 521-563.
(3) Adman, E. T.; Stenkamp, R. E.; Sieker, L. C.; Jensen, L. H. *J. Mol. Biol.* **1978**, *123*, 35-47.
(4) Solomon, E. I.; Hare, J. W.; Dooley, D. M.; Dawson, J. H.; Stephens, P. J.; Gray, H. B. *J. Am. Chem. Soc.* **1980**, *102*, 168-78.
(5) Beinert, H. *Coord. Chem. Rev.* **1980**, *33*, 55-85.

0002-7863/86/1508-1202$01.50/0